THE JOURNAL OF PHYSICAL CHEMISTRY A

A: Kinetics, Dynamics, Photochemistry, and Excited States

Cationic Dependence of X-ray Induced Damage of Strontium and Barium Nitrate

David Goldberger, Changyong Park, Egor Evlyukhin, Petrika Cifligu, and Michael Pravica

J. Phys. Chem. A, **Just Accepted Manuscript** • DOI: 10.1021/acs.jpca.8b08224 • Publication Date (Web): 19 Oct 2018

ACS Publications

is published by the American Chemical Society. 1155 Sixteenth Street N.W., Washington, DC 20036

Cationic Dependence of X-ray Induced Damage in Strontium and Barium Nitrate

*David Goldberger[1], Changyong Park[2], Egor Evlyukhin[1], Petrika Cifligu[1], Michael Pravica[1]**

[1]Department of Physics, University of Nevada Las Vegas (UNLV), Las Vegas Nevada 89154-4002, United States.

[2]High-Pressure Collaborative Access Team (HPCAT), Geophysical Laboratory, Carnegie Institution of Washington, Argonne, IL, 60439, USA

Abstract

The response of solids to x-ray irradiation is not well understood, in part, because the interactions between x-rays and molecules in solids depend on the intra- and/or inter-molecular electronic properties of the material. Our previous work demonstrated that x-ray induced damage of certain ionic salts depends on the irradiating photon energy, especially when irradiated with photons of energy near the cation's K-edge. To advance understanding of the cationic dependence of x-ray photochemistry, we present studies of x-ray induced damage of barium nitrate and strontium nitrate. Polycrystalline samples of barium and strontium nitrate were irradiated with high flux monochromatic synchrotron x-rays at selected energies near the K-edge of the respective cations. The damage processes were studied with powder x-ray diffraction, and irradiation products, NO_2 and O_2, were characterized via Raman spectroscopy. Our results demonstrate that irradiating barium and strontium nitrate with photons of energy greater than the K-edge of the cation promote a higher rate of decomposition compare to that observed when irradiating with photons of energy below the K-edge. Additionally, differences in x-ray induced damage between the two compounds are examined and discussed, and evidence of the diffusion of irradiation products is presented.

Introduction

Understanding x-ray induced stimuli, both chemical and structural, is crucial to many interdisciplinary fields. In astrobiology, x-ray-induced chemical reactions in the interstellar environment may lead to the formation of recently observed complex organic molecules[1]. In nuclear physics and weapons design, limiting long-term x-ray damage is critical to ensuring longevity and proper performance of systems[2-3]. In biology, x-ray-induced reactions lead to loss of functionality of biologically important molecules, particularly those containing metal centers[4-6]. In radiotherapy, x-ray-induced bond breaking reactions are employed to selectively kill cancerous cells[7-8]. Additionally, recent work in the developing field of *useful hard x-ray photochemistry* has shown that x-ray-induced chemical reactions can be harnessed and controlled to synthesize new compounds such as doped solid-CO[9], a new type of CsO_2[10], OF_2[11], and possibly CsF_2, and CsF_3[12]. Moreover, x-rays can be harnessed to produce simple molecules such as Cl_2[13], O_2[14], and even F_2[15], *in situ* inside of diamond anvil cells (DACs) for study at high pressure and to serve as reactants for further chemical reactions. X-rays have also been employed to dope semiconductors such as WO_3[16]. Better understanding of the mechanisms of x-ray photochemistry will improve the synthetic and decomposition control so that x-ray damages can be mitigated, and useful reactions can be harnessed.

Previous work has identified some of the characteristics of hard x-ray photochemistry, including a study of the products produced from the x-ray induced decomposition of barium and strontium nitrate[17]. However, to the best of our knowledge, no recent study has examined x-ray damage induced in solids by high flux sources such as synchrotrons. There is evidence, particularly from x-ray free electron laser (XFEL) experiments, that radiation-induced damage, when irradiating with high photon flux, is significantly different than with low flux[18]. Additionally, to

the best of our knowledge, few systematic studies have been conducted to characterize damage of solid materials as a function of irradiating photon energy[19-20]. Therefore, this study aims to investigate the radiation-energy-dependence of the damage process, and in addition, by comparison of x-ray damage induced in barium and strontium nitrates to ascertain cationic dependent aspects of the damage process.

Barium and strontium nitrate are ideal materials for this study. Each has a simple cubic structure, space group $Pa\bar{3}$, with lattice constants 8.118 and 7.781 Å, respectively[21]. Barium's K-edge is 37.414 keV whereas strontium's K-edge is 16.106 keV[22]. The probability of a nitrogen or oxygen atom interacting with an x-ray of ~16 keV or 37 keV energy is very low, due to their small absorption cross sections at such high energies[23]. This aids in understanding the stimuli in these systems as we can assume that the primary interaction is between the x-rays and the heavy cations. It is known that interaction between x-rays and heavy cations triggers many possible electronic relaxation processes[10, 24] that may lead to diverse results. By observing qualitative and quantitative differences between x-ray induced damage, we can offer insight into the mechanism governing high photon flux x-ray damage of ionic solids.

Experimental Section

All experiments were performed at the 16-BM-D beamline of the High-Pressure Collaborative Access Team (HP-CAT) at the Advanced Photon Source. Symmetric style DACs, with culets of 400-500 μm, were used in this experiment to provide a sealed and thermally conductive environment in which x-ray photochemistry could occur and be observed due to the optical transparency of diamond. Strontium and barium nitrate (99.0% and 99.9% Sigma Aldrich respectively) were separately loaded into stainless steel gaskets indented to ~30 μm and drilled on

the laser micro-machining system at HP-CAT[25]. Samples were pressurized to less than 0.5 GPa in all experiments. To expedite the loading of DACs inside a glovebox, gaskets were laser drilled with two or three sample chambers, each about 80 μm in diameter as displayed in Fig. 1. The sample chambers were symmetrically placed about the center of the diamond-diamond axis so that they pressurize similarly upon compression. A ruby sphere was loaded into each sample chamber for pressure measurements and no pressure transmitting medium was used. Upon pressurization, a pressure difference of 10-20% between sample chambers in the same gasket was measured[26]. The 16-BMD beamline provided monochromatic x-rays with tunable energies from 6-45 keV. The flux of the beam varies with energy - typically it is about 5×10^{8} photons/s on the sample. The resolution of the monochromator also varies but it is better than $\Delta E/E\leq10^{-3}$ for all energies studied[27]. X-ray flux was recorded by an ion chamber placed directly upstream of the sample and corrected for diamond absorption at different energies to determine the flux of photons incident on the sample at each energy. The X-ray beam was focused so that its FWHM was about 5×5 μm, though the beam profile varies as a function of energy as well. Powder X-ray diffraction (XRD) patterns were collected every minute over an hour of irradiation with a MAR345® image plate detector. The 2D diffraction patterns were reduced to intensities as a function of 2-theta angles using the Dioptas® program[28], which were then converted to intensity *versus* d-space plots via Bragg's law. *In-situ* Raman spectroscopy was performed on samples at room temperature before and after an hour of irradiation to characterize the obtained irradiation products.

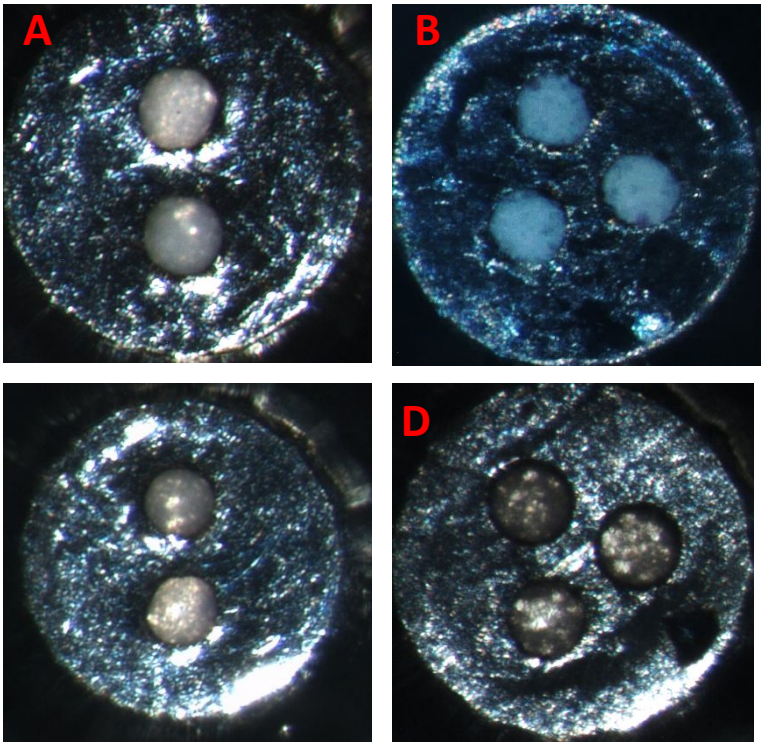

Figure 1. Samples of barium nitrate loaded in stainless-steel gaskets indented to ~30 μm and drilled on the laser micro-machining system. (A, B) pressurized in DAC, before irradiation, (C) pressurized in DAC after an hour of irradiation at 34 keV (top) and 36 keV (bottom), (D) after an hour of irradiation at 38, 40, and 42 keV (clockwise from top left). Note the dark tint of light transmitted through the samples irradiated at higher energy.

Results and Discussion

Visual Evidence

Pictures of samples of barium nitrate pressurized in a DAC both before and after irradiation at various energies are presented in Fig. 1. After an hour of irradiation with higher energy (i.e. above the Ba K-edge) photons, light transmitted through the samples is tinted brown (see Fig. 1(D)), however no change is observed at lower energies below the Ba K-edge (see Fig. 1(A, C)). The visible change of the tint of transmitted light through the sample is the first evidence that a reaction has taken place. The lack of visible changes to the sample when irradiating at energy below the K-edge of barium suggests that x-ray damage proceeds differently above and below the

K-edge. To further elucidate these differences, and to identify the irradiation products we investigated the samples via Raman spectroscopy.

Raman Spectroscopy

Fig. 2 displays *in-situ* Raman Spectra of barium and strontium nitrate before and after x-ray irradiation at selected energies which are above or below the respective cation's K-edge. The spectra of barium and strontium nitrate before irradiation both exhibit strong peaks at ~745 and ~1055 cm^{-1} as well as a small shoulder at ~1400 cm^{-1} on the diamond peak (1332 cm^{-1}), as previously reported[29]. These peaks correspond to the in-plane bend, the symmetric stretch, and the antisymmetric stretch of the NO_3^- anion respectively. Post-irradiation Raman spectra exhibit slight but critical differences when compared to pre-irradiation spectra.

For both strontium and barium nitrate, Raman spectra obtained after irradiating with higher energy (above-K-edge) x-rays clearly show two new peaks at ~840 and ~1560 cm^{-1}. These new peaks are much less apparent or non-existent in the low energy (below-K-edge) Raman spectra. The new peak near 840 cm^{-1} can either be assigned to the O-O stretch mode in a mixture of MO_2 and MO (M = Ba or Sr)[30] or to the bending mode of NO_2^- [17]. The new peak around 1560 cm^{-1} can be assigned to the well-known O-O vibrational stretch mode in O_2 [31]. The appearance of these new peaks in the Raman spectra corroborate previous findings that irradiation of solid anhydrous nitrates leads to decomposition according to the reaction[17]:

$$2NO_3^- \rightarrow 2NO_2^- + O_2 \quad (1)$$

After the initial decomposition of the nitrate anion, the system is left in a highly-energetic, unstable state and further relaxation may lead to the creation of various molecular species including NO_2, O_2, MO, MO_2, etc. that could not be distinguished based on Raman spectroscopy. Visual evidence suggests that one of the irradiation products is NO_2 gas which is likely

responsible for the brown tint of light transmitted through the post-irradiation samples (see Fig. 1(D)). The fact that the entire sample chamber exhibits the same visual change, despite the relatively minute (5×5 μm) x-ray beam incident on the sample suggests that the NO_2, or other undetermined product, released upon irradiation is highly mobile under these conditions. A similar finding was reported for the mobility of oxygen upon irradiation of $KClO_4$ [32].

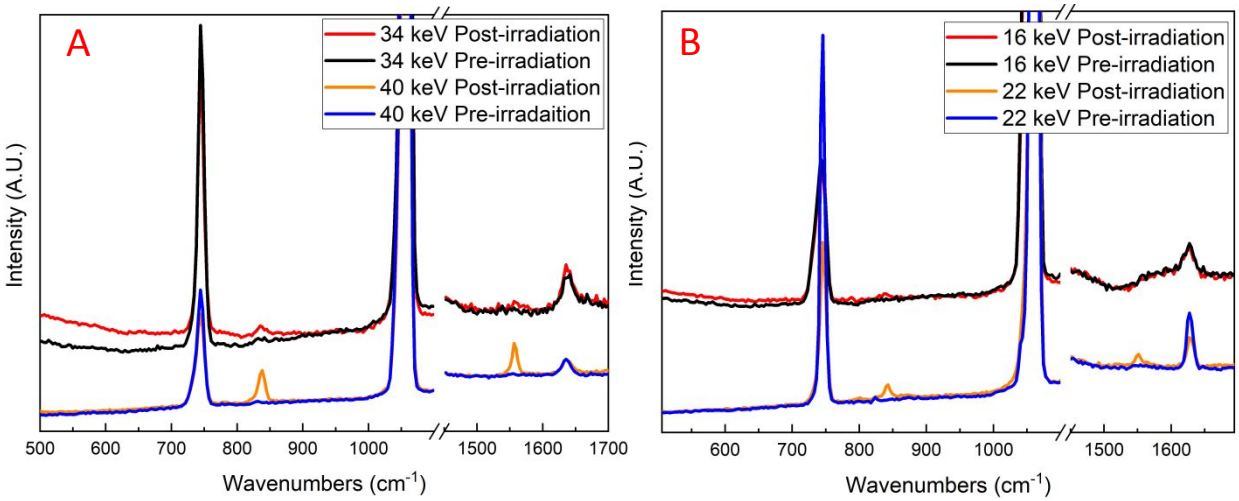

Figure 2. Pre- and post-irradiation Raman spectra of (A) barium and (B) strontium nitrate. Note the appearance of new peaks in the higher-energy, post-irradiation spectra.

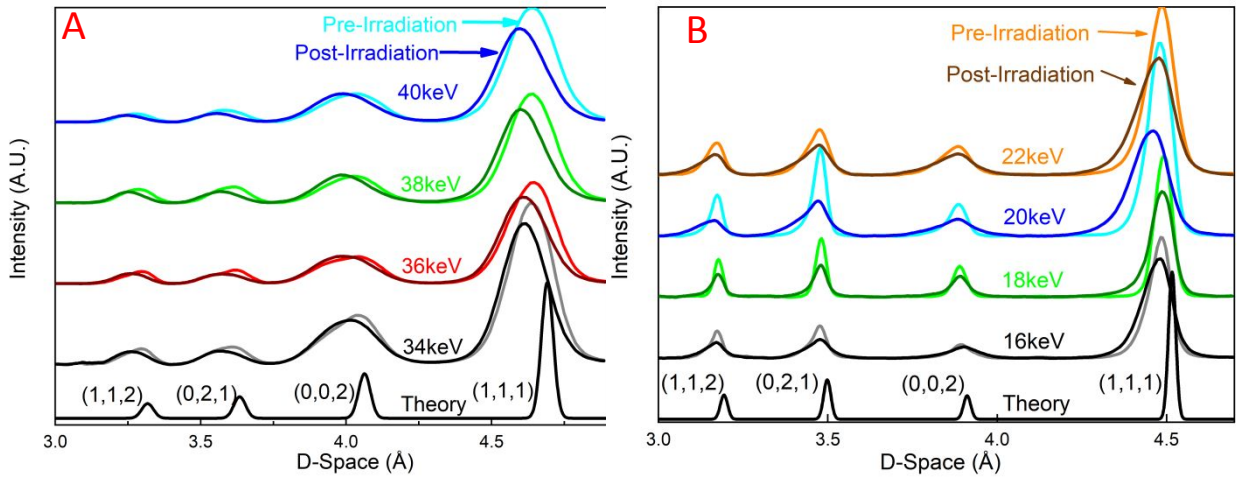

Figure 3. Pre- and post-irradiation diffraction patterns of (A) barium and (B) strontium nitrate. Patterns are stacked and colored by energy, and light colors indicate pre-irradiation patterns while dark colors indicate post-irradiation patterns. We observe three qualitative changes of peaks in diffraction patterns: integrated area changes, peak center shifts, and peak width changes.

X-ray Diffraction

Fig. 3 presents *in situ* powder x-ray diffraction patterns obtained before and after irradiation for studied energies of (a) barium and (b) strontium nitrate. It should be noted that the diffraction peaks in the pre-irradiation patterns are already shifted to lower d-space by roughly the same small amount (~1% relative to the theoretical patterns). This indicates that the samples were all stressed to modest, similar pressures.

Comparison of the diffraction patterns obtained before and after irradiation demonstrates the effect of x-ray induced damage. Subtle alterations of the post-irradiation diffraction patterns indicate physical changes of the samples. Three aspects of each diffraction peak appear to change: the integrated area of the peak, the position of the peak center and the full width at half maximum (FWHM) of the peak. However, the degree to which each of these parameters varies over the course of irradiation depends on the energy of the irradiating photons and on the sample itself. To elucidate these differences, we quantitively examine each of these features.

To quantify changes of the diffraction peaks over the course of irradiation we fit each clearly distinguishable peak to a Gaussian and extract the integrated area, FWHM, peak center, and the error for each of these parameters[33]. Each parameter is normalized to its initial value for the given peak and energy, and the percent change as a function of fluence, is determined by:

$$\text{"\%Change of X"(F)} \equiv 100\% * \left(\frac{\text{X(F)}}{\text{X(0)}} - 1\right) \quad (2)$$

This normalization is necessary to ensure that we are accurately comparing percent change when irradiating with different photon energies and when comparing parameters of different peaks. The data is presented as a function of fluence, rather than as a function of irradiation time, to accurately compare observed percent change when irradiating with different photon flux.

The first feature that we examined is the integrated area of diffraction peaks. Based on previous work on x-ray-induced decomposition of strontium oxalate[20], a percent change of integrated area of a diffraction peak is indicative of atomic dislocations in the crystal lattice, which result in reduced diffraction signal. We propose that the main driver of atomic dislocations in the studied systems is the decomposition of nitrate anion and subsequent relaxation and diffusion processes. As the decomposition process dislocates atoms from their stable lattice positions, diffraction peaks reduce in intensity. Thus, we quantify the decomposition yield (DY) of our sample as:

$$\mathrm{DY(F)} = 100\% * \left(1 - \frac{\text{Peak Area(F)}}{\text{Peak Area (0)}}\right) \quad (3)$$

We calculated the DY for selected diffraction peaks and then averaged them to obtain the results presented in Fig 4. As we are averaging over diffraction peaks that represent different planes within the crystal lattice, it is possible that the change of integrated area of selected peaks will be different depending on the atomic configurations in Bragg planes. Therefore, when the average decomposition yields as calculated in Eqn. 3 results in a negative value of DY, we interpret this as indicative of a reordering of the powder crystalline lattices within the sample, as opposed to strict decomposition. This reordering leads to an increase of diffraction peak intensity and thus produces a negative DY.

When irradiating barium nitrate at energies (34 keV and 36 keV) below the barium K-edge, (see Fig. 4(a)) the average DY initially decreases providing slightly negative values and subsequently increases to modest decomposition yields (~ 5%). The initial decrease of DY suggests a reordering of the powder crystalline lattices. We suspect that this reordering is caused by x-ray induced relaxation of local strain initially introduced by uniaxial sample compression. Relaxation of strain and decomposition are then two competing x-ray induced processes that affect

the observed DY, and their interplay can be seen in the oscillations of DY. Above the barium K-edge, the DY increases more dramatically, and maximum DY (~10%) is achieved when irradiating with photons of higher energy. A similar comparison can be made with strontium nitrate (see Fig 4(b)). When irradiating with photons of energy below the strontium K-edge (16 keV), the average DY is similarly modest (~5%). As in the previous case, when irradiating above the K-edge, the DY is higher. Both systems show that the DY is higher when irradiating with photon energy greater than the cation's K-edge, which is in agreement with the previously reported study of x-ray induced decomposition of strontium oxalate[20].

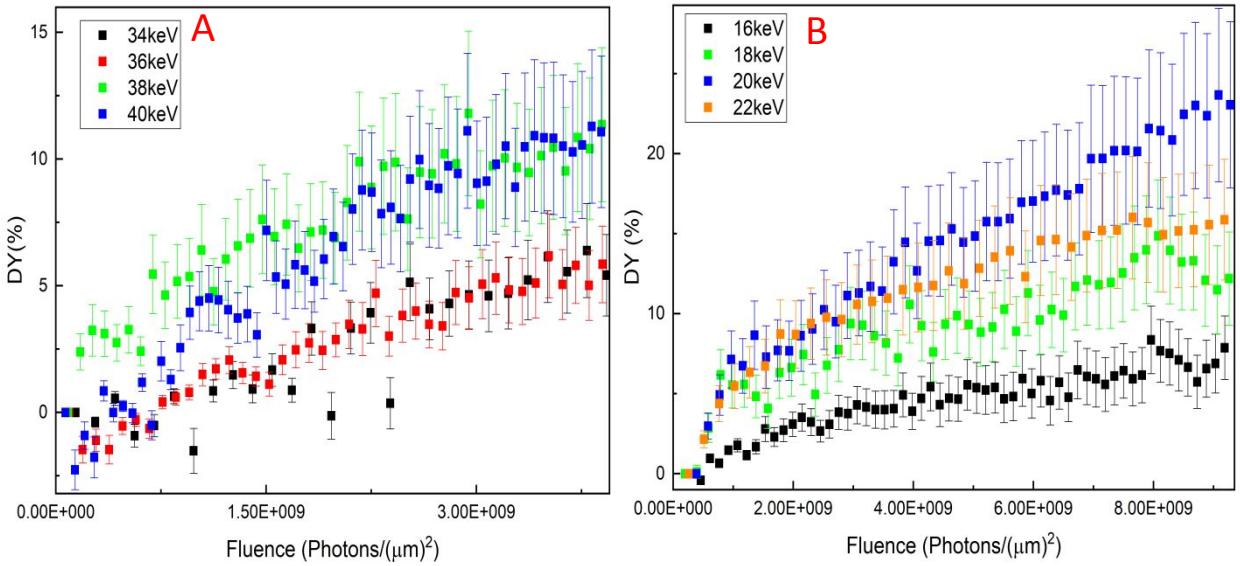

Figure 4. The average Decomposition Yield (DY) as a function of fluence for (A) barium and (B) strontium nitrate. The average is taken over selected peaks and the error bars indicate the standard deviation of the average.

To gain further insight into the mechanism of x-ray induced damage, we studied the changes in FWHM of selected diffraction peaks. The factors that cause broadening of diffraction peaks can be divided into two main categories: instrumental and sample contribution. For our experimental setup the instrumental contributions are small (< 1%) and constant at each energy[27], thus we can conveniently neglect them. The sample contributions to broadening can further be broken down into either size broadening or strain broadening factors[34]. Basically, smaller crystal

grains and crystals that have greater inhomogeneous strain will give broader diffraction peaks. Thus, an increase in peak widths indicates either decreasing grain size or increasing inhomogeneous strain. These changes likely occur because of the production of mobile molecular species like NO_2 and O_2, which upon escaping from the crystal lattice can break apart large grains or leave voids that increase inhomogeneous strain in the sample.

Fig. 5 displays the average changes in the FWHM measured over selected diffraction peaks. The effect of irradiation is significantly different in the two systems studied. In strontium nitrate (see Fig. 5(b)), irradiation leads to similar dramatic increase (~20-40%) of the final FWHM of peaks at all energies, except at 20 keV where the increase is even more dramatic (~90%). Whereas in barium nitrate (see Fig. 5(a)), irradiation below the K-edge leads to slight increase of FWHM (~5%), while irradiation above the K-edge leads to slight decrease of FWHM (~3%). Except for the 20 keV strontium nitrate case, the trend in change is opposite that found in the average DY. The irradiated samples were more decomposed above the K-edges while inhomogeneous strains were suppressed under the same condition. This further indicates that a localized process of relaxation of the strained lattice was triggered simultaneously with the radiation-induced decomposition process.

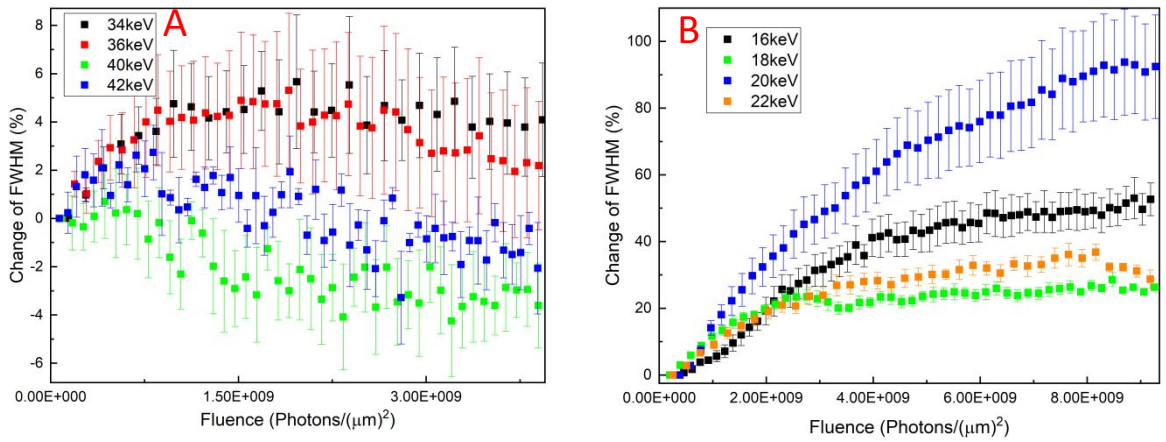

Figure 5. The average percent change of full width half maximum (FWHM) of peaks as a function of fluence for (A) barium and (B) strontium nitrate. The average is taken over selected peaks and the error bars indicate the standard deviation.

The last parameter that we analyzed was the diffraction peak center shift. A shift of a diffraction peak indicates homogeneous strain[34], which is characterized by a change of the unit cell lattice parameter(s). Since both barium and strontium nitrate have simple cubic structure, their unit cells are described by only one lattice parameter, *a*. For the cubic structure, the percent volume change of the unit cell can be calculated from the cubic d-spacing of a peak as:

$$\%\ \text{Volume (F)} = 100\% * \left(\frac{\text{d(F)}}{\text{d(0)}}\right)^3 \quad (4)$$

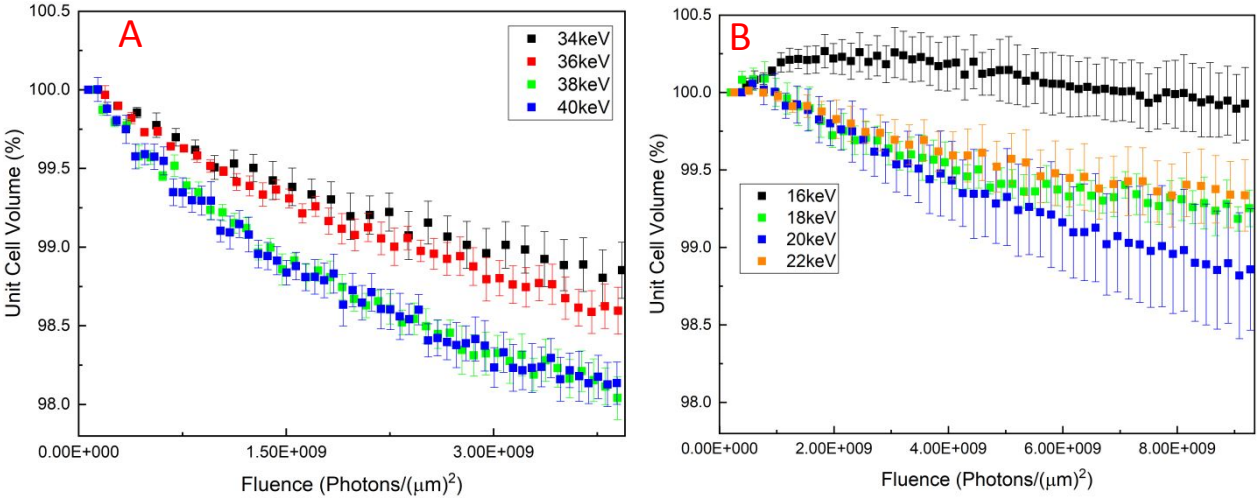

Figure 6. The average unit cell volume for (A) barium and (B) strontium nitrate as a function of fluence. The average is taken over selected peaks and the error bars indicate the standard deviation.

Fig. 6 displays the average unit cell volume recorded over selected peaks at each studied energy as a function of fluence. For barium nitrate (see Fig. 6(a)) the unit cell volume monotonically decreases at all energies over the course of x-ray irradiation. Above the barium K-edge the decrease of the unit cell volume is more dramatic than below the barium K-edge. A similar trend was observed in the case of barium nitrate DY as presented in Fig. 4(a). When irradiating strontium nitrate (see Fig. 6(b)) the unit cell volume initially increases slightly and then decreases. This effect appears most prominently when irradiating with 16 keV photons, but it is noticeable for all energies. Like barium nitrate, irradiating strontium nitrate above its K-edge leads to significant decrease of the unit cell volume, however irradiating strontium and barium nitrate below their respective K-edges yields significantly different responses. The reduction of unit cell volume observed upon irradiation corroborates the production of free molecular species as detected visually. Breakdown of the NO_3 anion and subsequent escape of NO_2 and/or O_2 gas leads to decreasing volume. Due to the presence of a pressure gradient in the sample, free/mobile species such as O_2 diffuse from the interaction region of the x-ray beam where they are created, as observed in Figure 1D.

The similarities and differences between the results for barium and strontium nitrate may help to elucidate the mechanism of x-ray induced damage. Visual evidence, results from Raman spectroscopy, and analysis of XRD patterns (DY, FWHM, and unit cell volume) demonstrate cation-specific dependence of x-ray induced damages. The above-K-edge post-irradiation Raman spectra show new peaks that are not apparent, or much less significant, in the below-K-edge post-irradiation spectra. From the XRD patterns, we observe that irradiation above the cations K-edge leads to greater decomposition, and more significant reduction in the unit cell volumes. These

results corroborate our previous findings of the energy dependence of x-ray induced decomposition of strontium oxalate[20]. However, the behavior of peak widths showed somewhat different and more complicated processes. The FWHM after above-K-edge irradiation showed reduced inhomogeneous lattice strains compared to that after below-K-edge irradiation, except for 20 keV irradiation on strontium nitrate. These results, and the initially negative DY observed at low fluence, indicate a simultaneous local lattice relaxation process accompanying radiation-induced decomposition. The trend of FWHM with increasing fluency also deviated for the barium and strontium nitrate cases, which we infer would be related to fundamental differences in unit cell packing or photon-atom interactions.

Over the course of irradiation, the FWHM of strontium nitrate peaks continuously increase, whereas the FWHM of barium nitrate peaks vary differently depending on the energy of x-ray irradiation (see Fig. 5), and they change less overall. We propose two plausible physical interpretations of this difference. First, since barium is larger than strontium, the unit cell packing of barium nitrate is less sensitive to the decomposition of the nitrate anion. Thus, as decomposition and diffusion proceed, there is less buildup of inhomogeneous strain in the barium nitrate unit cell, so diffraction peaks do not broaden as significantly. A second physical interpretation is that the absorption cross section of strontium at the studied energies is about two times higher than that of barium[23]. Higher absorption cross section suggests that the probability for strontium atoms to absorb x-ray photons at the studied energies is higher than that of barium atoms and possibly related to the higher rate of decomposition (Fig.4). The latter, in turn, may be related to the far enhanced FWHM changes in strontium nitrate with increasing fluency (Fig. 5), which further indicates the FWHM trend with fluency would be the result of competition of two opposing effects: generating new defects vs. relaxing local strains. It is an interesting point that radiation-induced

stimuli likely consist of both destructive and constructive processes that are in competition. Based on these preliminary results, further studies that can separate these competing effects may lead to further control of x-ray photochemistry, making it an even more powerful tool.

Conclusion

We have performed systematic studies of x-ray induced damage of barium and strontium nitrate as a function of the energy of the irradiating photons. Comparison of pre and post-irradiation Raman spectroscopy, as well as visual evidence, indicate that, for both systems, irradiating with photons of energy greater than the K-edge of the cation leads to decomposition of the material and production of NO_2 and O_2 gas. Irradiating with photons of energy less than the K-edge leads to less significant decomposition and less or no production of NO_2 and O_2. Analysis of the XRD patterns obtained over the course of irradiation suggests that irradiating above the K-edge of the cations leads to larger decomposition yield and greater reduction of unit cell volumes, for both systems. These findings corroborate those in previous work, and further evidence the cationic dependence of x-ray induced damage of ionic salts. Furthermore, we have evidence that some irradiation products become highly mobile under the studied conditions and their diffusion may be directly related to changing aspects of x-ray diffraction patterns. Future studies will aim to use similar techniques to study molecular diffusion at extreme conditions.

Additionally, comparison of the FWHM of diffraction peaks over the course of irradiation suggest that the cation's absorption cross section and the photon flux of the irradiating beam play important roles in x-ray induced damage. It is strongly suspected that two independent, competing processes, i.e., decomposition and local strain relaxation, are simultaneously triggered by irradiation, and that these effects may exhibit different responses to changing cationic absorption cross section or photon flux. While this requires further investigation, we propose that we may

gain further control of x-ray induced processes by considering systems with cations of various absorption cross sections, or by modulating the photon flux of the irradiating beam This control will be critical to *useful hard x-ray photochemistry*, as well as myriad related disciplines.

Corresponding Author

Michael Pravica - Pravica@physics.unlv.edu

Present Address for CP

High-pressure Collaborative Access Team, X-ray Science Division, Argonne National Laboratory, Argonne, IL 60439, USA

Conflicts of Interest

There are no conflicts of interest to declare.

Acknowledgements

We gratefully acknowledge support from the Department of Energy National Nuclear Security Administration (DOE-NNSA) under Award Number DE-NA0002912. We also acknowledge support from the DOE Cooperative Agreement No. DE-FC08-01NV14049 with the University of Nevada, Las Vegas. C.P. acknowledges the support of DOE-BES/DMSE under award DE-FG02-99ER45775. Portions of this work were performed at HPCAT (Sector 16), Advanced Photon Source (APS), Argonne National Laboratory. HPCAT operation is supported by DOE-NNSA under Award No. DE-NA0001974, with partial instrumentation funding by the NSF. The Advanced Photon Source is a U.S. Department of Energy (DOE) Office of Science User Facility operated for the DOE Office of Science by Argonne National Laboratory under Contract No. DE-AC02-06CH11357.

References

(1) McGuire, B. A.; Burkhardt, A. M.; Kalenskii, S.; Shingledecker, C. N.; Remijan, A. J.; Herbst, E.; McCarthy, M. C., Detection of the aromatic molecule benzonitrile (c-C6H5CN) in the interstellar medium. *Science* **2018,** *359*, 202-205.
(2) Giefers, H.; Pravica, M., Radiation-induced decomposition of PETN and TATB under extreme conditions. *J. Phys. Chem. A* **2008,** *112*, 3352-3359.
(3) Giefers, H.; Pravica, M.; Liermann, H.P.; Wang, Y., Radiation-induced decomposition of PETN and TATB under pressure. *Chem. phys. lett.* **2006,** *429*, 304-309.
(4) Jawad, H.; Watt, D., Physical mechanism for inactivation of metallo-enzymes by characteristic X-rays. *Int. J. Radiat. Biol.* **1986,** *50*, 665-674.
(5) Yano, J.; Kern, J.; Irrgang, K.D.; Latimer, M. J.; Bergmann, U.; Glatzel, P.; Pushkar, Y.; Biesiadka, J.; Loll, B.; Sauer, K., X-ray damage to the Mn4Ca complex in single crystals of photosystem II: a case study for metalloprotein crystallography. *Proc. Natl. Acad. Sci. U.S.A.* **2005,** *102*, 12047-12052.
(6) Takakura, K., Double-strand breaks in DNA induced by the K-shell ionization of calcium atoms. *Acta Oncol.* **1996,** *35*, 883-888.
(7) Martin, R. F.; Feinendegen, L. E., The quest to exploit the Auger effect in cancer radiotherapy–a reflective review. *Int. J. Radiat. Biol.* **2016,** *92*, 617-632.
(8) Biston, M.C.; Joubert, A.; Adam, J.F.; Elleaume, H.; Bohic, S.; Charvet, A.M.; Estève, F.; Foray, N.; Balosso, J., Cure of Fisher rats bearing radioresistant F98 glioma treated with cis-platinum and irradiated with monochromatic synchrotron X-rays. *Cancer Res.* **2004,** *64*, 2317-2323.
(9) Pravica, M.; Evlyukhin, E.; Cifligu, P.; Harris, B.; Koh, J. J.; Chen, N.; Wang, Y., X-ray induced synthesis of a novel material: Stable, doped solid CO at ambient conditions. *Chem. Phys. Lett.* **2017,** *686*, 183-188.
(10) Evlyukhin, E.; Kim, E.; Goldberger, D.; Cifligu, P.; Schyck, S.; Weck, P. F.; Pravica, M., High-pressure-assisted X-ray-induced damage as a new route for chemical and structural synthesis. *Phys. Chem. Chem. Phys.* **2018**, *20*, 18949-18956.
(11) Pravica, M.; White, M.; Wang, Y., A novel method for generating molecular mixtures at extreme conditions: The case of fluorine and oxygen. *AIP Conf. Proc.* **2017,** *1793*, 060030.
(12) Maosheng, M.; Jorge, B.; Michael, P.; Daniel, S.; Changyong, P., Inner-shell chemistry under high pressure. *Jpn. J. Appl. Phys.* **2017,** *56*, 5S3.
(13) Pravica, M.; Sneed, D.; Smith, Q.; Bai, L., High pressure X-ray photochemical studies of carbon tetrachloride: Cl2 production and segregation. *Chem. Phys. Lett.* **2013,** *590*, 74-76.
(14) Pravica, M.; Wang, Y.; Sneed, D.; Reiser, S.; White, M., High pressure studies of potassium perchlorate. *Chem. Phys. Lett.* **2016,** *660*, 37-42.
(15) Pravica, M.; Bai, L.; Park, C.; Liu, Y.; Galley, M.; Robinson, J.; Bhattacharya, N., Note: A novel method for in situ loading of gases via x-ray induced chemistry. *Rev. Sci. Instrum.* **2011,** *82*, 106102.
(16) Michael, P.; Yonggang, W.; Yuming, X.; Paul, C.; Yonggang, W.; Yuming, X.; Paul, C., High pressure resonant X-ray emission studies of WO and hydrogenated WO. *JJAP Conf. Proc.* **2017,** *011102*, 6.
(17) Cunningham, J.; Heal, H., The decomposition of solid nitrates by X-rays. J. Chem. Soc. Faraday Trans. **1958,** *54*, 1355-1369.
(18) Rudenko, A.; Inhester, L.; Hanasaki, K.; Li, X.; Robatjazi, S. J.; Erk, B.; Boll, R.; Toyota, K.; Hao, Y.; Vendrell, O.; et al. Femtosecond response of polyatomic molecules to ultra-intense hard X-rays. *Nature* **2017,** *546*, 129-132.
(19) Pravica, M.; Bai, L.; Sneed, D.; Park, C., Measurement of the energy dependence of x-ray-Induced decomposition of potassium chlorate. *J. Phys. Chem. A* **2013,** *117*, 2302-2306.
(20) Goldberger, D.; Evlyukhin, E.; Cifligu, P.; Wang, Y.; Pravica, M., Measurement of the energy and high-pressure dependence of x-ray-Induced decomposition of crystalline strontium oxalate. *J. Phys. Chem. A* **2017,** *121*, 7108-7113.

(21) Nowotny, H.; Heger, G., Structure refinement of strontium nitrate, Sr (NO3) 2, and barium nitrate, Ba (NO3) 2. *Acta Crystallogr. C* **1983,** *39*, 952-956.
(22) Thompson, A.; Attwood, D.; Gullikson, E.; Howells, M.; Kim, K. J.; Kirz, K.; Kortright, J.; Lindau, I.; Liu, Y.; Pianetta, P.; et al. *X-ray Data Booklet;* Lawrence Berkeley National Laboratory: **2009**.
(23) McMaster, W. H.; Del Grande, N. K.; Mallett, J. H.; Hubbell, J. H. *Compilation of X-Ray Cross Sections;* Lawrence Livermore National Laboratory: **1969**.
(24) Stumpf, V.; Gokhberg, K.; Cederbaum, L. S., The role of metal ions in X-ray-induced photochemistry. *Nat. Chem.* **2016,** *8*, 237-241.
(25) Hrubiak, R.; Sinogeikin, S.; Rod, E.; Shen, G., The laser micro-machining system for diamond anvil cell experiments and general precision machining applications at the High Pressure Collaborative Access Team. *Rev. Sci. Instrum.* **2015,** *86*, 072202.
(26) Zhao, J.; Hearne, G.; Maaza, M.; Nieuwoudt, M. K.; Comins, J. D., Multi-aperture gasket for experiments at high pressure in a diamond-anvil cell. *Rev. Sci. Instrum.* **2000,** *71*, 4509-4511.
(27) Park, C.; Popov, D.; Ikuta, D.; Lin, C.; Kenney-Benson, C.; Rod, E.; Bommannavar, A.; Shen, G., New developments in micro-X-ray diffraction and X-ray absorption spectroscopy for high-pressure research at 16-BM-D at the Advanced Photon Source. *Rev. Sci. Instrum.* **2015,** *86*, 072205.
(28) Prescher, C.; Prakapenka, V. B., DIOPTAS: a program for reduction of two-dimensional X-ray diffraction data and data exploration. *High Pressure Res.* **2015,** *35*, 223-230.
(29) Zverev, P. G.; Murray, J. T.; Powell, R. C.; Reeves, R. J.; Basiev, T. T., Stimulated Raman scattering of picosecond pulses in barium nitrate crystals. *Opt. Commun.* **1993,** *97*, 59-64.
(30) Waal, D. d.; Range, K. J.; Königstein, M.; Kiefer, W., Raman spectra of the barium oxide peroxide and strontium oxide peroxide series. *J. Raman Spectrosc.* **1998,** *29*, 109-113.
(31) Hill, R.; Esherick, P.; Owyoung, A., High-resolution stimulated Raman spectroscopy of O2. *J. Mol. Spectrosc.* **1983,** *100*, 119-133.
(32) Pravica, M.; Popov, D.; Sinogeikin, S.; Sneed, D.; Guardala, G.; Smith, Q., X-ray induced mobility of molecular oxygen at extreme conditions. *Appl. Phys. Lett.* **2013,** *103*, 224103.
(33) Tracy, C. L.; Lang, M.; Pray, J. M.; Zhang, F.; Popov, D.; Park, C.; Trautmann, C.; Bender, M.; Severin, D.; Skuratov, V. A.; et al. Redox response of actinide materials to highly ionizing radiation. *Nat. Commun.* **2015,** *6*, 6133.
(34) Young, R. A. *The Rietveld Method*. Oxford University Press: **1993**.

TOC Graphic:

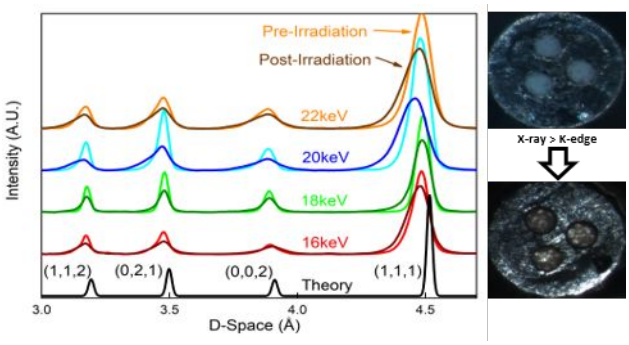
Pre-Irradiation
Post-Irradiation
22keV
20keV
18keV
16keV
(1,1,2)
(0,2,1)
(0,0,2)
Theory
(1,1,1)
Intensity (A.U.)
3.0
3.5
4.0
4.5
D-Space (Å)
X-ray > K-edge